IPPI

Polyolefins Journal, Vol. 8, No. 2 (2021)
DOI: 10.22063/poj.2021.2795.1169

ORIGINAL PAPER

Ethylene yield in a large-scale olefin plant utilizing regression analysis

Mohamad Hafizi Zakria[1,2,*], Mohd Ghazali Mohd Nawawi[1], Mohd Rizal Abdul Rahman[2,3], Mohd Anas Saudi[2]

[1]School of Chemical and Energy Engineering, Faculty of Engineering, Universiti Teknologi Malaysia, 81310, Johor, Malaysia
[2]Steam Cracker Complex, Manufacturing Division, Pengerang Refining Company Sdn Bhd, PICMO B2, Pengerang Integrated Complex, 81600, Johor, Malaysia
[3]Group Technical Solutions, Petroliam Nasional Berhad (PETRONAS), The Intermark Tower, 55000 Kuala Lumpur, Malaysia

Received: 25 October 2020 , Accepted: 19 May 2021

ABSTRACT

The research was carried out in a large-scale olefin process to see how different variables affect ethylene yield in an actual fluctuating plant condition. Regression analysis was adopted using Minitab Software Version 18 to create a reliable ethylene yield model. Regression analysis is a robust, practical, and advanced tool that is used in various applications as an alternative to the complex, expensive, and restricted simulation software that is specifically designed for the olefin process. The 1688 data taken from the studied plant underwent outliers and residuals removal utilizing normality and stability tools in Minitab for the analysis to be conducted as normal data. The Regression was conducted a few times until all variables satisfactorily met the multicollinearity criteria with Variance Inflation Factor (VIF) <10 and 95% confidence level criteria with P-Value <0.05. The final Regression model established 4 significant variables which were Hearth Burner Flow, Integral Burner Flow, Super High-Pressure Steam (SHP) Temperature, and Naphtha Feed Flow by factors of -0.001266, 0.04515, -0.0795, and 0.2105, respectively. The maximum ethylene yield was calculated at 31.75% using Response Optimizer with the recommended operating conditions at 9908.50 kg/h Hearth Burner Flow, 600.39 kg/h Integral Burner Flow, 494.65°C SHP Temperature, and 63.50 t/h Naphtha Feed Flow. **Polyolefins J (2021) 8: 105-113**

Keywords: Olefin yield; steam cracker furnace; optimization; statistical analysis; Minitab.

INTRODUCTION

The research was carried out in a newly commissioned olefin plant that used naphtha liquid as a feedstock to the steam cracker furnace. The plant was designed to produce 1,100 KTA of polymer grade ethylene through pyrolysis cracking in a steam cracker furnace. It is challenging to undertake the study in real plant scale conditions due to the typical process fluctuation [1-3] in a large application. This is due to various controlled and uncontrolled variables continuously affecting the process, especially resulted from feedstock impurities, utility reliability and influence of upstream/downstream plant performance. The studied plant was constructed at a mega-scale petroleum complex with full integration to the upstream and downstream plant

*Corresponding Author - E-mail: mohamadhafizi.zakri@prefchem.com

where the process fluctuation is frequent and cannot be fully prevented.

Pyrolysis cracking involves a high-temperature firing in the steam cracker furnace [4, 5] that allows hydrocarbon bonds to break and generates the smaller and unsaturated molecule [6, 7] of olefin products like ethylene, propylene and butylene. Olefin plants that use thermal cracking technology are unique in the way that they are typically regarded as the heart of the petrochemical industry [8, 9], and their performances signify the growth of the petrochemical industry in the country [10].

Lummus, Linde, Stone and Webster, M.W. Kellogs, Technip [11, 12], and Sinopec [13, 14] are examples of the established Olefin Licensors which having mature, reliable, and proven olefin technologies. Olefin Licensors own the proprietary steam cracker furnace design and usually offer their simulation software such as SPYRO [15, 16], SHAHAB [17], CRACKER [18, 19], CHEMKIN [20-22], and CRACKSIM [23-25] to the olefin plants worldwide. Although these software are undeniably robust, they are more complex, expensive, and also restricted in some applications to safeguard the proprietary design by Olefin Licensors.

The generation of ethylene from pyrolysis cracking in the Short Residence Time (SRT) VII furnace is one of the most promising technologies currently available in the market [26, 27]. Figure 1 portrays the configuration of the studied SRT VII and its auxiliaries used for the study.

The naphtha feed enters the furnace through the first bank of the convection section, where it will

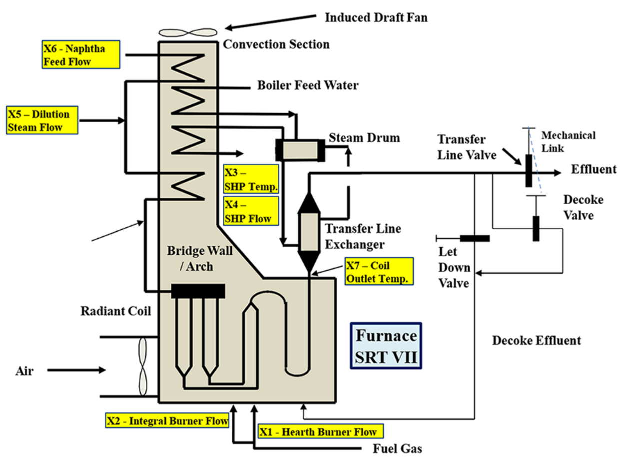

Figure 1. SRT VII configuration with the selected 7 variables for the study.

combine with Dilution Steam (DS) to increase olefin selectivity by lowering the partial pressure of naphtha feed [28, 29]. This mixing initiated to favor a better ethylene yield from the reversible reaction according to Le Chatelier's Principles [30, 31]. The initial dynamic equilibrium is broken by the introduction of DS to the naphtha feed. The place of equilibrium changes to compensate for the adjustment and therefore, reestablishment of equilibrium starts. When a chemical reaction is at equilibrium and a change occurs, the equilibrium moves in the opposite direction to compensate for the change following the Le Chatelier’s Principle.

This mixed feed will then flow into the radiation section with the operated 1,050°C-1,180°C of Tube Metal Temperature (TMT) at radiant coils. This extreme temperature is essential to maximize the ethylene yield in the SRT VII. The cracked gas will then be sent to the downstream equipment for further quenching, compression, cooling and product separation.

The steam cracker furnace is one of the critical equipment in the olefin process [32] where its performance determines the yield and quality of ethylene produced [33]. This translates to the profit generation for the olefin plant. However, the rapid cracking of naphtha feed in the furnace coils will lead to the formation of coke over time and it cannot be avoided due to the extreme cracking temperature in the SRT VII. The decoke cycle is therefore critical for removing hard coke from the furnace coil.

To ensure continuous ethylene generation [34] and sustainable normal cracking conditions [35] for the furnaces, a mixture of air and steam is used for decoke operation according to the scheduled period that is planned earlier by operations personnel. The mechanical link between Decoke Valve and Transfer Line Valve shown in Figure 1 is utilized for this purpose. Maintaining safe and stable operation [36, 37] including during decoke cycle is crucial to ensure continuation of naphtha cracking in the SRT VII.

This study is significant in showing the result of robust Regression analysis in the actual large-scale olefin plant where process fluctuation is normally observed. The final Regression model is important to portray the actual olefin plant performance with consideration to the various fluctuating variables in the large-scale olefin process. It also provides practical alternatives to the complex simulation software by Olefin Licensors that is normally applied in the Olefin plant. In summary, Regression analysis is easier, cheaper, and has no proprietary restrictions on the statistical software used.

EXPERIMENTAL

Equipment/Tools

The study utilized 93 t/h of naphtha feed processing capacity of SRT VII furnace designed by Lummus Technology Heat Transfer (LTHT), United States. Process Information Management System (PIMS) Software, PI Process Book Version 2015 was used to collect plant data for the selected variables, and Minitab Software Version 18 was employed to perform the whole analysis.

Methodology

7 variables were chosen with consideration to the: a) major input/output control, b) firing intensity and c) main temperature parameters, as those were the most critical variables for the Steam Cracker Furnace operation. In this case, the input was Naphtha Feed, and the output was Ethylene Yield. The variables controlling the firing intensity to the furnace were Hearth Burner Flow and Integral Burner Flow. The main temperature parameters for the analysis were Super High Pressure (SHP) Flow, SHP Temperature, and Coil Outlet Temperature (COT). These 7 variables were also the most important parameters frequently observed in the studied plant to monitor the Ethylene Yield and therefore were selected into the Regression analysis for this study.

The date for the study was set on the 24th of January 2020, 1700 h to the 2nd of February 2020, 1200 h with an accumulated 211 h. The data was collected hourly (calculated average, time-weighted) from the PI Process Book. There was a total of 1,688 data points used for the analyses represented by 7 inputs and 1 output.

The Paraffins, Olefins, Naphtenes, Aromatics (PONA) compositions in the naphtha feed were 60.92 vol%, 1.02%, 25.97%, and 12.09%, respectively, with the Initial Boiling Point (IBP) and Final Boiling Point (FBP) which were 34.1ºC and 166.1°C, respectively. The Reid Vapour Pressure (RVP) was 44.5 kPa. The naphtha feed specification was ensured not exceeding 5% of variance to ensure that the final model was representative of the constant naphtha feed specification throughout the study duration.

All 1,688 data were initially analyzed using 5 tools in Minitab Software Version 18 to determine the data normality and stability. The data stability was first verified using three different tools which were Box Plot, Run Chart and Individual-Moving Range (I-MR) Chart. The normality verification continued after the stability test completion using the Normality Plot and Graphical Summary.

The normality distribution test followed symmetry around the mean and could be classified based on mean and standard deviation. It was important to ensure that the data were normal using the normality test before Regression analysis started. The stability test referred to the process that stayed stable during the study cycle, implying that the process produced consistent performance at all times. It plotted the data over time and used local dispersion measures to estimate within-process variance, enabling it to detect deviations from natural process variation. Unstable processes could be non-normal, and non-normal processes could be stable. Both tests were therefore essential to ensure the data credibility in this continuous process condition.

The P-Value in both the stability and normality should be verified greater than 0.05 to continue with Regression analysis as normal data. If the P-Value provided by these tools was less than 0.05, the analysis would be conducted using Box-Cox data transformation. However, it was not intended to undergo data transformation in this study, and therefore it was necessary to pass both tests. P-Value higher than 0.05 is the worldwide recognized figure for the statistical analysis. Although the study was conducted in the fluctuating process condition, 0.05 was also selected for this study to comfortably provide the 95% of confidence level for the final model. The low P-Value showed solid proof against the null hypothesis, as the null hypothesis had less than 5% chance of being right and the model was therefore established from the reliable and well-distributed data. However, there was no need to undergo the P-Value less than 0.05 as per normal practices in the biotechnology field which often requires more sensitive analysis.

The Regression was repeated a few times, eliminating one variable at a time until all variables had a VIF of <10 and a P-Value of <0.05. The series of variable elimination began with the highest VIF value and continued until all variables had a VIF of 10 or less. In an ordinary least squares regression analysis, VIF measures the severity of multicollinearity that existed in the model. VIF >10 was not recommended [38] because it could influence the P-value and contributed to the inaccurate model. VIF <5 was also recommended [39] because it further reduced the multicollinearity in the Regression model. However, VIF <10 was adequate in this study due to the nature of analysis at the large-scale plant condition with numerous process variations.

After all remaining variables achieved VIF <10, the variable elimination continued for the variable with the highest P-Value until all variables achieved P-Values of 0.05 or less. Once both of VIF and P-Value criteria were met, the Residual elimination was performed on the most recent Regression model using the Fit and Diagnostic for Unusual Observation table. After removing all residues, the Regression was reconducted to all 7 variables. The same approach was reconducted to improve the model and to eliminate the insignificant variables that did not meet VIF and P-Value criteria.

The scatterplot of input versus output of ethylene yield was drawn to see the normal distribution of the model and its R-Square. Finally, the Response Optimizer tool was also applied to the final model to predict the maximum value of ethylene yield with the significant process settings that can be accomplished in the studied plant.

RESULTS AND DISCUSSION

Table 1 shows the initial (1st) and final (7th) Regression analysis results, while Eq. 1 demonstrates the final equation model after the 7th Regression.

$$Y1 = 43.1 - 0.001266\,(X1) + 0.04515\,(X2) - 0.0795\,(X3) + 0.2105\,(X6) \quad (1)$$

The 1st Regression was conducted to establish the initial relation between all studied variables. The VIFs for all variables were successfully obtained at <5 in the 1st Regression and therefore no variable was eliminated from the initial Regression due to high VIF. The 2nd and 3rd Regression were conducted with the removal of variables with P-Value >0.05. The elimination started with X5 (P-Value: 0.378) and was followed by X4 (P-Value: 0.272). All remaining variables X1, X2, X3, X6, and X7 had successfully obtained P-Value <0.05 in the 3rd Regression with the R-Square observed at 70.58%.

However, 19 residuals were still observed on the Fits and Diagnostic for Unusual Observations table. These residuals were therefore removed, and the 4th Regression was reconducted to all variables to improve the model.

The 5th to 7th Regressions were conducted with the sequence of removal started from X4 (P-Value: 0.517), X7 (P-Value: 0.311), and X5 (P-value: 0.097). The R-Square for the 7th Regression was observed at 76.43% which is higher than the 3rd Regression by 5.85%. Although all variables in the 3rd Regression were found at P-Value <0.05, removing the residuals from regression analysis significantly improved the model by 5.85% in the 7th Regression.

Table 1 shows that all variables achieved the VIF of <5 since the initial Regression. This displayed

Table 1. Initial and final Regression analysis for all variables.

Tag and Description		Unit	Initial Regression (1st)			Final Regression (7th)		
			Coef.	P-Value	VIF	Coef.	P-Value	VIF
Constant			-55.7	0.079		43.1	0.003	
X1	**Hearth Burner Flow**	kg/h	-0.001020	0.000	4.67	-0.001266	0.000	4.88
X2	**Integral Burner Flow**	kg/h	0.05169	0.000	1.42	0.04515	0.000	1.83
X3	**SHP Temperature**	°C	-0.0435	0.025	2.30	-0.0795	0.003	1.53
X4	**SHP Flow**	t/h	-0.0310	0.252	2.33			
X5	**Dilution Steam Flow**	kg/h	-0.000117	0.378	1.04			
X6	**Naphtha Feed Flow**	t/h	0.1864	0.000	3.16	0.2105	0.000	3.54
X7	**Coil Outlet Temp.**	ºC	0.1030	0.011	1.47			

Table 2. Model summary.

S	R-sq	R-sq(adj)	R-sq(pred)
0.205502	76.43%	75.85%	74.75%

that very minimal multicollinearity relations existed between 7 identified variables used for the Regression analysis. It was also an indication of the good variable selection for the reliable final equation model.

The final model built from the study is summarized in Table 2. Given that the analysis was performed in the actual large-scale plant where process variation was common, the R-Square value of 76.43% was excellent. It demonstrated 76.43% of the variability was considered in the final model. This value was also sufficient to justify the data variability, which was recommended at 75% or higher [40, 41].

Figure 2 shows the normality distribution of the Y1 (Ethylene Yield) based on the input and output values. The high R-Square of 76.43% in the scatterplot portrayed the reliable input data in achieving the output from the final model. Although the trend showed that small data fell into the 30% - 31% range compared to the majority within the 28.5% - 29.5% range; it was acceptable as the study being conducted in the actual plant scale condition supported by the high R-Square at 76.43%.

Figure 3 displays the Contour Plot for the significant variables in the final Regression model. The Y1 (Ethylene Yield) was mapped with the prediction

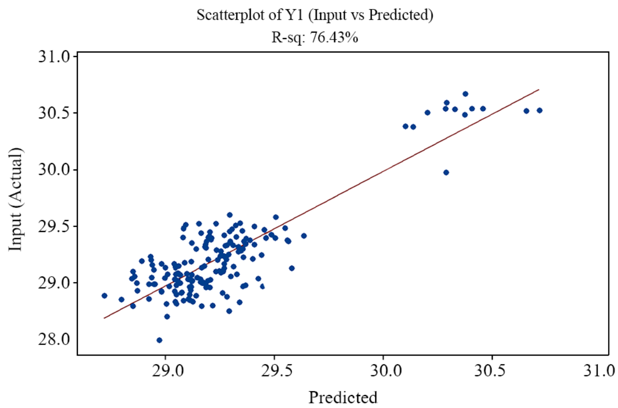

Figure 2. Normal data distribution of input Y1 versus output Y1.

value of <28.5% – >30.5%.

The relation between X2 (Integral Burner Flow) versus X1 (Hearth Burner Flow) had the greatest effect in achieving the highest Y1 (Ethylene Yield) at >30.5%. The higher X2 (Integral Burner Flow) reading combined with the lower X1 (Hearth Burner Flow) demonstrated the highest Y1 (Ethylene Yield) result with the biggest contour range of >30.5%. The relation of these two parameters was therefore critical to be observed by the studied plant to achieve the best Y1 (Ethylene Yield). Besides, X3 (SHP Temperature) versus X1 (Hearth Burner Flow) and X6 (Naphtha Feed Flow) versus X1 (Hearth Burner Flow) relations also displayed the existence of Y1 (Ethylene Yield) range at >30.5%.

Figure 3 also showed X3 (SHP Temperature) versus X2 (Integral Burner Flow), X6 (Naphtha Feed Flow)

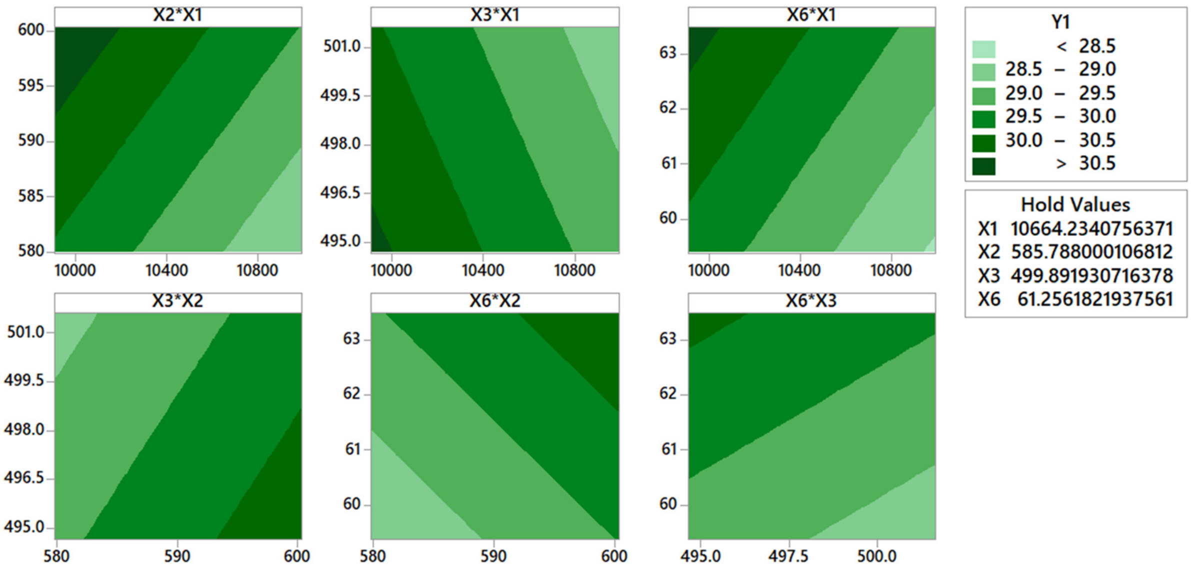

Figure 3. Contour plot of the relationship between significant variables in the final model in achieving Y1; X1, X2, X3, and X6.

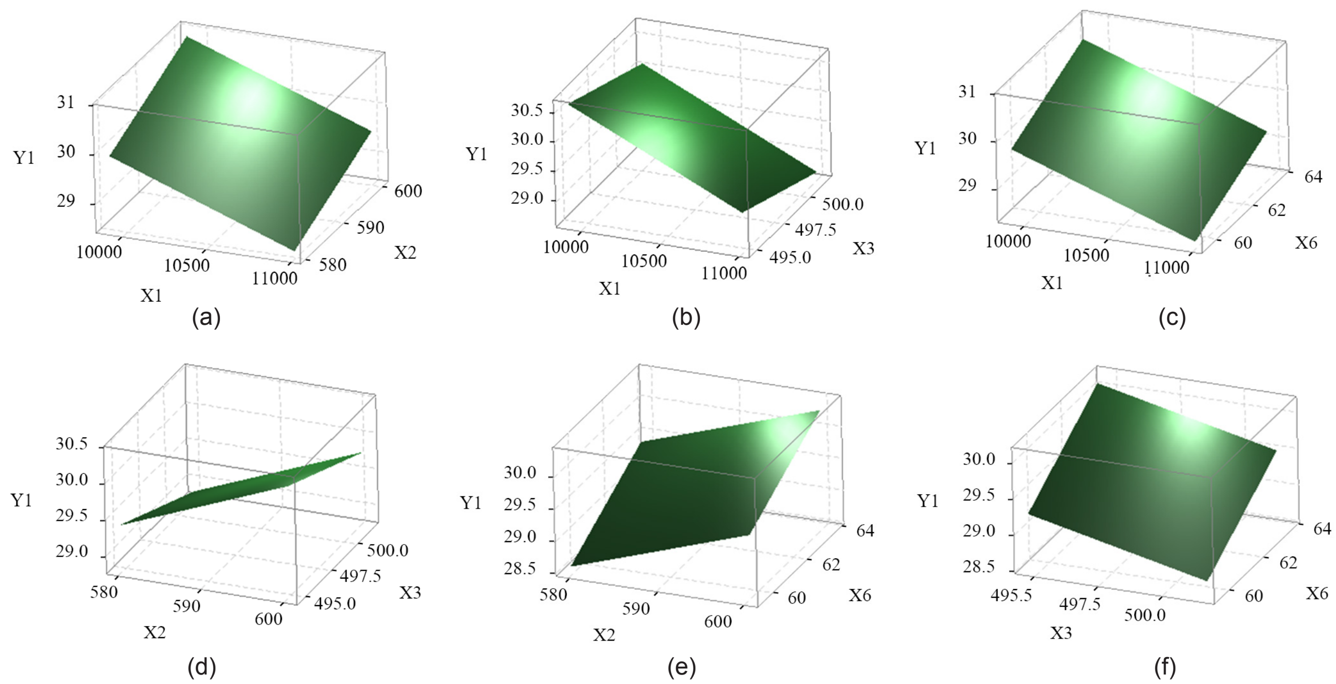

Figure 4. Surface plot for Y1 against the identified variables in the final model; (a) X1 vs X2, (b) X1 vs X3, (c) X1 vs X6, (d) X2 vs X3 (e) X2 vs X6 and (f) X3 vs X6.

versus X2 (Integral Burner Flow), and X6 (Naphtha Feed Flow) versus X3 (SHP Temperature) relations were not much favor towards higher Y1 (Ethylene Yield). This was presented by no contour range observed at >30.5% of Y1 (Ethylene Yield) between these relations.

The Surface Plot of significant variables in comparison to Y1 (Ethylene Yield) is shown in Figure 4. This 3D Surface Plot is a three-dimensional graph that can be used to investigate desirable response values for two continuous variables centered on the model equation against Y1 (Ethylene Yield). The mean value for non-tested variables was held at 10664.23 kg/h, 585.79 kg/h, 499.89ºC, and 61.26 t/h for X1 (Hearth Burner Flow), X2 (Integral Burner Flow), X3 (SHP Temperature), and X6 (Naphtha Feed Flow), respectively.

From the Surface Plot in Figure 4 (a) and Figure 4 (c), the lower value of X1 (Hearth Burner Flow) combined with the higher value of X2 (Integral Burner Flow), and X6 (Naphtha Feed Flow) resulted in higher Y1 (Ethylene Yield). The same combination was also observed in Figure 4 (f) between X3 (SHP Temperature) and X6 (Naphtha Feed Flow). These combinations were also critical to achieve the highest Y1 (Ethylene Yield) as the graph peak approaching the top of the Surface Plot.

Furthermore, lower X3 (SHP Temperature) combined with lower X1 (Hearth Burner Flow) or higher X2 (Integral Burner Flow) will also result in higher Y1 (Ethylene Yield) as shown in Figure 4 (b) and Figure 4 (d). Finally, Figure 4 (e) displays higher X2 (Integral Burner Flow) was required to be operated with the higher X6 (Naphtha Feed Flow) to establish the better Y1 (Ethylene Yield). In general, the Surface Plot helped to show the 3D relations between each variable as a guide to the Operations personnel to maximize the Y1 (Ethylene Yield). However, the 2D Contour Plot in Figure 3 presented the operating condition to achieve the Y1 (Ethylene Yield) within the desired range in a simpler form.

Table 3. Response prediction for the final Regression model.

Response	Fit	SE Fit	Confidence	
			95% CI	95% PI
Y1	31.751	0.131	(31.493, 32.009)	(31.270, 32.232)

Table 3 displays the Multiple Response Prediction, while Figure 5 depicts the use of the Response Optimizer to set the best operating condition to maximize Y1 (Ethylene Yield).

The Y1 (Ethylene Yield) was calculated to be

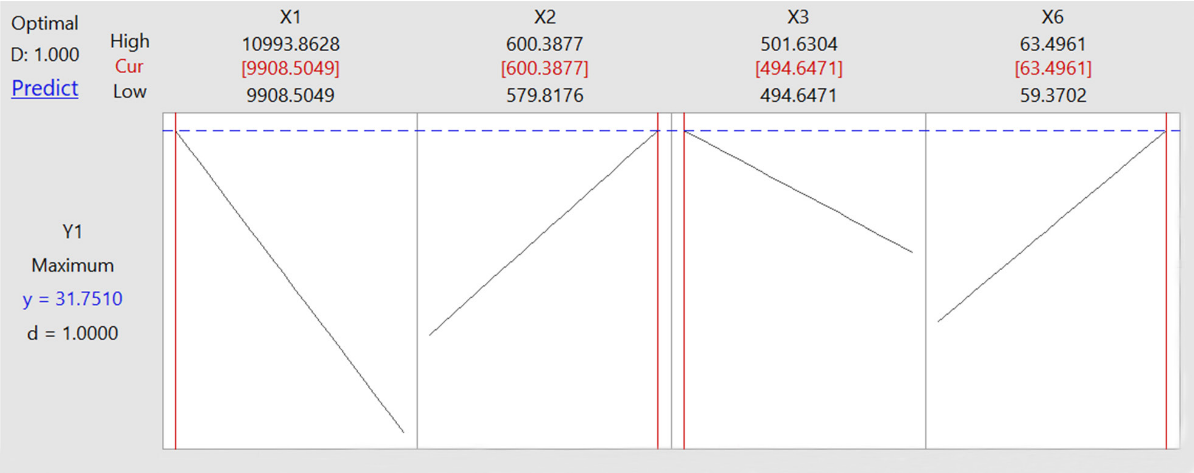

Figure 5. Operating condition for significant variables to achieve maximum Y1 from Response Optimizer.

maximized at 31.75% with the recommended operating conditions at 9,908.50 kg/h of Hearth Burner Flow, 600.39 kg/h of Integral Burner Flow, 494.65°C of SHP Temperature, and 63.50 t/h of Naphtha Feed Flow. The low and high range setting for significant variables in the Response Optimizer may also be used as a reference for the Operations personnel in the studied plant to maximize the Y1 (Ethylene Yield).

CONCLUSION

The final Regression model summarized 4 significant variables to maximize Ethylene Yield at 31.75% which were Hearth Burner Flow, Integral Burner Flow, SHP Temperature, and Naphtha Feed Flow, with the factor of -0.001266, 0.04515, -0.0795, and 0.2105, respectively. This study successfully closed the gaps for the easier and practical olefin yield evaluation adopting the Regression analysis as the alternative to the normally applied complex, expensive and restricted olefin simulation software. The model also proved reliable from the high R-Square at 76.43% regardless of the study being conducted in the fluctuating process conditions.

ACKNOWLEDGEMENTS

The authors are grateful to Steam Cracker Complex, Pengerang Refining Company Sdn Bhd for excellent industrial assistance in completing the report. In addition, special gratitude is also dedicated to the Faculty of Engineering, Universiti Teknologi Malaysia for the academic assistance in preparing this paper.

Symbol and Abbreviation

COT	Coil Outlet Temperature
DS	Dilution Steam
FBP	Final Boiling Point
I-MR	Individual-Moving Range
IBP	Initial Boiling Point
KTA	Kilo Tonne Per Annum
LTHT	Lummus Technology Heat Transfer
PIMS	Process Information Management System
PONA	Paraffins, Olefins, Napthenes, Aromatics
RVP	Reid Vapor Pressure
SHP	Super High Pressure
SRT	Short Residence Time
TLE	Transfer Line Exchanger
TMT	Tube Metal Temperature
VIF	Variance Inflation Factor

REFERENCES

1. Zakria MH, Omar AA, Bustam MA (2016) Mercury removal of fluctuating athane feedstock in a large scale production by sulphur impregnated activated carbon. Procedia Eng 148: 561-567
2. Feli Z, Darvishi A, Bakhtyari A, Rahimpour MR, Raeissi S (2017) Investigation of propane addition to the feed stream of a commercial

ethane thermal cracker as supplementary feedstock. J Taiwan Inst Chem Eng 81: 1-13

3. Zakria MH, Mohd Ghazali MN, Abdul Rahman MR (2021) Ethylene yield from a large scale naphtha pyrolysis cracking utilizing response surface methodology. Pertanika J Sci Technol 29: 791-808
4. Shi H, Su C, Cao J, Li P, Liang J, Zhong G (2015) Nonlinear adaptive predictive functional control based on the Takagi–Sugeno model for average cracking outlet temperature of the ethylene cracking furnace. Ind Eng Chem Res 54: 1849-1860
5. Song H, Su C-l, Shi H, Li P, Cao J-t (2019) Improved predictive functional control for ethylene cracking furnace. Meas Control 52: 526-539
6. Van de Vijver R, Vandewiele N, Bhoorasingh P, Slakman B, Seyedzadeh Khanshan F, Carstensen HH, Reyniers MF, Marin B, West R, Van Geem K (2015) Automatic mechanism and kinetic model generation for gas- and solution-phase processes: A perspective on best practices, recent advances, and future challenges. Int J Chem Kinet 47: 199-231
7. Vangaever S, Reyniers PA, Symoens SH, Ristic ND, Djokic MR, Marin GB, Van Geem KM (2020) Pyrometer-based control of a steam cracking furnace. Chem Eng Res Design 153: 380-390
8. Fan T-J, Luo R, Xia H, Li X (2015) Using LMDI method to analyze the influencing factors of carbon emissions in China's petrochemical industries. Nat Hazards 75: 319-332
9. Nikolaidis IK, Franco LFM, Vechot LN, Economou IG (2018) Modeling of physical properties and vapor – liquid equilibrium of ethylene and ethylene mixtures with equations of state. Fluid Ph Equilibria 470: 149-163
10. Gong S, Shao C, Zhu L (2017) Energy efficiency evaluation based on DEA integrated factor analysis with respect to operation classification in ethylene production. Chin J Chem Eng 25: 793-799
11. Brayden M, Hines D, Graham J, Pickett T (2008) Top 5 contaminants in ethylene production unit feedstock. In: 2012 AIChE Annual Meeting. AIChE, New Orleans, Lousiana
12. Sadrameli SM (2015) Thermal/catalytic cracking of hydrocarbons for the production of olefins: A state-of-the-art review I: Thermal cracking review. Fuel 140: 102-115
13. Wang Z, Han Y, Li C, Geng Z, Fan J (2021) Input-output networks considering graphlet-based analysis for production optimization: Application in ethylene plants. J Clean Prod 278: 123955
14. Pu X, Shi L (2013) Commercial test of the catalyst for removal of trace olefins from aromatics and its mechanism. Catal Today 212: 115-119
15. Dente M, Ranzi E, Goossens AG (1979) Detailed prediction of olefin yields from hydrocarbon pyrolysis through a fundamental simulation model (SPYRO). Comput Chem Eng 3: 61-75
16. Van Goethem MWM, Kleinendorst FI, van Leeuwen C, van Velzen N (2001) Equation-based SPYRO® model and solver for the simulation of the steam cracking process. Comput Chem Eng 25: 905-911
17. Toufighi J, Karimzadeh R, Saedi G, Hosseini S, Morafahi M, Mokhtarani B, Niaee A, Sadr AM (2004) SHAHAB-A PC-based software for simulation of steam cracking furnaces (ethane and naphtha). Iran J Chem Eng 1: 55-70
18. Joo E, Lee K, Lee M, Park S (2000) CRACKER - a PC based simulator for industrial cracking furnaces. Comput Chem Eng 24: 1523-1528
19. Joo E, Park S (2001) Pyrolysis reaction mechanism for industrial naphtha cracking furnaces. Ind Eng Chem Res 40: 2409-2415
20. Kee RJ, Rupley FM, Miller JA, Coltrin ME, Grcar JF, Meeks E, Moffat HK, Lutz AE, Dixon-Lewis G, Smooke MD (2006) CHEMKIN Release 4.1. Reaction Design
21. Reyniers PA, Schietekat CM, Kong B, Passalacqua A, Van Geem KM, Marin GB (2017) CFD simulations of industrial steam cracking reactors: Turbulence–chemistry interaction and dynamic zoning. Ind Eng Chem Res 56: 14959-14971
22. Van Cauwenberge DJ, Vandewalle LA, Reyniers PA, Van Geem KM, Marin GB, Floré J (2017)

Periodic reactive flow simulation: Proof of concept for steam cracking coils. AIChE J 63: 1715-1726

23. Hillewaert LP, Dierickx JL, Froment GF (1988) Computer generation of reaction schemes and rate equations for thermal cracking. AIChE J 34: 17-24
24. Van Geem K, Reyniers M, Marin G (2008) Challenges of modeling steam cracking of heavy feedstocks. Oil Gas Sci Technol 63: 79-94
25. Willems PA, Froment GF (1988) Kinetic modeling of the thermal cracking of hydrocarbons. 1. Calculation of frequency factors. Ind Eng Chem Res 27: 1959-1966
26. Caballero DY, Biegler LT, Guirardello R (2015) Simulation and optimization of the ethane cracking process to produce ethylene. Comput Aided Chem Eng 37: 917-922
27. Kuritsyn V, Arapov D, Ekimova A, Yakupov A (2008) Modeling of pyrolysis of straight-run naphtha in a large-capacity type SRT-VI furnace. Chem Technol Fuels Oils 44: 180-189
28. Karimi H, Cowperthwaite E, Olayiwola B, Farag H, McAuley K (2017) Modelling of heat transfer and pyrolysis reactions in an industrial ethylene cracking furnace. Can J Chem Eng 96: 33-48
29. Masoumi M, Sadrameli SM, Towfighi J, Niaei A (2006) Simulation, optimization and control of a thermal cracking furnace. Energy 31: 516-527
30. Cai Y, Yang S, Fu S, Zhang D, Zhang Q (2017) Investigation of Portevin–Le Chatelier band strain and elastic shrinkage in Al-based alloys associated with Mg contents. J Mater Sci Technol 33: 580-586
31. Epstein LG (1978) The Le Chatelier principle in optimal control problems. J Econ Theory 19: 103-122
32. Junfeng Z, Zhiping P, Delong C, Qirui L, Jieguang H, Jinbo Q (2019) A method for measuring tube metal temperature of ethylene cracking furnace tubes based on machinelearning and neural network. IEEE Access 7: 158643-158654
33. Wang Z, Li Z, Feng Y, Rong G (2016) Integrated short-term scheduling and production planning in an ethylene plant based on Lagrangian decomposition. Can J Chem Eng 94: 1723-1739
34. Kucora I, Paunjoric P, Tolmac J, Vulovic M, Speight J, Radovanovic L (2017) Coke formation in pyrolysis furnaces in the petrochemical industry. Pet Sci Technol 35: 213-221
35. Sun X, Shen L (2017) Research progress of coking mechanism and prevention measures for ethylene cracking furnace tubes. Corros Sci Prot Technol 29: 575-580
36. Peng Z, Zhao J, Yin Z, Gu Y, Qiu J, Cui D (2019) ABC-ANFIS-CTF: A method for diagnosis and prediction of coking degree of ethylene cracking furnace tube. Processes 7: 909
37. Shen L, Gong J, Liu H (2015) Effect of coking size on the thermal diffusion and stress distribution of $Cr_{25}Ni_{35}Nb$ and $Cr_{35}Ni_{45}Nb$ austenitic steels. Appl Mech Mater 750: 192-197
38. Hair JF, Anderson RE, Tatham RL, Black WC (1995) Multivariate data analysis with readings. Prentice-Hall
39. Ringle C, Wende S, Becker J-M (2015) SmartPLS 3. Bönningstedt: SmartPLS. Retrieved from http://www.smartpls.com
40. Haaland PD (1989) Experimental design in biotechnology. Marcel Dekker, New York
41. Wan Omar WNN, Nordin N, Mohamed M, Saidina Amin NA (2009) A two-step biodiesel production from waste cooking oil: Optimization of pre-treatment step. J Appl Sci 9: 3098-3103